



Paclitaxel/methotrexate co-loaded PLGA nanoparticles in glioblastoma treatment: Formulation development and in vitro antitumor activity evaluation



Fatemeh Madani^a, Seyedeh Sara Esnaashari^b, Maria Camilla Bergonzi^c, Thomas J. Webster^d, Husam M. Younes^e, Masood Khosravani^{a,*}, Mahdi Adabi^{a,*}

^a Department of Medical Nanotechnology, School of Advanced Technologies in Medicine, Tehran University of Medical Sciences, Tehran, Iran

^b Department of Medical Nanotechnology, Faculty of Advanced Sciences and Technology, Tehran Medical Sciences, Islamic Azad University, Tehran, Iran

^c Department of Chemistry, University of Florence, Via U. Schiff 6, 50019 Sesto Fiorentino, Florence, Italy

^d Chemical Engineering Department, Northeastern University, Boston, MA 02115, USA

^e Office of Vice President For Research & Graduate Studies, Qatar University, Doha, Qatar

ARTICLE INFO

Keywords:

Paclitaxel
Methotrexate
PLGA
Co-delivery
Glioblastoma
Nanoparticles

ABSTRACT

Aim: The aim of this study was to improve the therapeutic index of chemotherapeutic drugs on glioblastoma cells through an improved co-drug delivery system.

Materials and methods: Methotrexate (MTX) and paclitaxel (PTX) were co-loaded into poly (lactic-co-glycolic acid) nanoparticles (PLGA NPs) coated with polyvinyl alcohol (PVA) and Poloxamer188 (P188).

Key findings: The mean size of the NPs was about 212 nm, with a zeta potential of about -15.7 mV. Encapsulation efficiency (EE%) and drug loading (DL%) were determined to be 72% and 4% for MTX and 85% and 4.9% for PTX, respectively. The prepared NPs were characterized by differential thermal analysis (DTA) and thermogravimetric analysis (TGA). Moreover, an in vitro sustained release profile was observed for both drug loaded PLGA NPs. Glioblastoma cellular uptake of the NPs was confirmed by fluorescence microscopy and cell survival rate was investigated through the 3-(4,5-dimethyl thiazol-2-yl)-2,5-diphenyltetrazolium bromide (MTT) method after 48 h of incubation showing IC_{50} values of $24.5 \mu\text{g}\cdot\text{mL}^{-1}$ for PTX and $9.5 \mu\text{g}\cdot\text{mL}^{-1}$ for MTX for the MTX/PTX co-loaded PLGA nanoparticles coated with PVA/P188 (Co-2 NPs). Apoptosis and necrosis were also studied via flow cytometry, the lactate dehydrogenase (LDH) assay and the amount of anti-apoptotic protein (Bcl-2) expression. Blood compatibility of the co-delivery of PTX and MTX loaded PLGA NPs was investigated using a hemolysis method as well.

Significance: The co-delivery of PTX and MTX loaded PLGA NPs is promising for the treatment of glioblastoma compared to their respective free drug formulations and, thus, should be further investigated.

1. Introduction

Despite the development of chemotherapeutic drugs for inhibiting the growth of cancer cells, drug penetration into the central nervous system and across the blood-brain barrier (BBB) has remained an

unsolved problem to date [1]. To overcome this challenge, nanocarriers are good choices, because they better penetrate into the brain due to their unique small properties and with large surface to volume ratios, leading to enhanced chemotherapeutic efficiency. One of the most significant problems in the clinic is organ failure due to conventional

Abbreviations: BBB, blood-brain barrier; MTX, methotrexate; PTX, paclitaxel; PVA, polyvinyl alcohol; P188, Poloxamer188; DL, drug loading; DLS, dynamic light scattering; DTA, differential thermal analysis; EE, encapsulation efficiency; GM, glioblastoma multiform; PLGA, poly(lactic-co-glycolic acid); TGA, thermogravimetric analysis; Co-1 NPs, MTX/PTX co-loaded PLGA nanoparticles coated with PVA; Co-2 NPs, MTX/PTX co-loaded PLGA nanoparticles coated with PVA/P188; Mix free, mixture of free MTX and free PTX; Mix NPs, mixture of MTX NP2 and PTX NP2; MTT, 3-(4,5-dimethyl thiazol-2-yl)-2,5-diphenyltetrazolium bromide; MTX NP1, MTX loaded PLGA nanoparticles coated with PVA; MTX NP2, MTX loaded PLGA nanoparticles coated with PVA/P188; NP, PLGA nanoparticles without any coating; NP1, PLGA nanoparticle coated with PVA; NP2, PLGA nanoparticles coated with PVA/P188; PTX NP1, PTX loaded PLGA nanoparticles coated with PVA; PTX NP2, PTX loaded PLGA nanoparticles coated with PVA/P188

* Corresponding authors.

E-mail addresses: drkhosravani@tums.ac.ir (M. Khosravani), madabi@tums.ac.ir (M. Adabi).

<https://doi.org/10.1016/j.lfs.2020.117943>

Received 31 March 2020; Received in revised form 3 June 2020; Accepted 8 June 2020

Available online 10 June 2020

0024-3205/ © 2020 Published by Elsevier Inc.

chemotherapy resulting from untargeted distribution and accumulation of chemotherapeutic agents in healthy organs, such as the liver, spleen, kidney, heart, etc. Therefore, targeted drug delivery needs to be developed to reduce the amount of chemotherapeutic agents required to kill cancer cells [2].

Drug delivery with targeting ligands can augment nanoparticle passage across the BBB [3,4] with Poloxamer188 (Pluronic® F-68) and polysorbate80 further serving as targeting ligands to the central nervous system [2,5]. One mechanism explaining this facilitation of the transport can be provided by the absorption of apolipoproteins onto a nanoparticle' surface, enhancing endogenous targeting. Therefore, using such approaches, nanoparticles can enter endothelial cells in the BBB by the assistance of such cell receptors [6].

Among the common drugs used in the clinic, PTX and MTX are some of the most effective agents for cancer therapy. PTX as an antimetabolic agent and a hydrophobic drug, resulting in cell death through the disruption of the microtubule network organization inhibiting the late G2 phase and M phase of the cell cycle, stopping cell replication [7]. In addition, MTX (a folic acid analogue) can competitively inhibit the key enzyme of folic acid synthesis and prevent the synthesis of purines and pyrimidines, which decrease tumor cell growth [8]. Since each chemotherapeutic agent affects tumor cells at different parts of the cell cycle, the co-delivery of two or more therapeutically agents enhance their ability to stop tumor cells from dividing. As proof of this co-delivery promise, there is a report that a patient with incurable head and neck squamous cell carcinoma survived for 16 months with a chemotherapeutic regimen containing MTX, PTX and nimotuzumab [9]. According to the results from this treatment, it seems that these drugs are potent agents against this kind of tumor when prescribed together, however, more studies are needed to demonstrate their combined efficiency for all cancers, especially glioblastoma.

It is claimed that the co-delivery of chemotherapeutic agents can increase the level of therapeutic effects and decrease drug resistance in tumors using a complementary effect [10,11]. For example, Xiaomeng Wan et al. prepared polymeric micelles co-loaded with PTX and cisplatin for the treatment of ovarian and breast cancer [12]. Also, more specifically for glioblastoma, the authors of the present study published another prosperous study for the co-delivery of curcumin and MTX by PLGA nanoparticles, which resulted in a higher cytotoxic effect compared to the respective free drugs on U-87 MG cells [13].

The objective of this study was, therefore, to prepare PTX/MTX loaded PLGA nanoparticles modified with PVA and P188 and determine the toxicity, cellular uptake, apoptosis and necrosis effect of these nanoparticles on a model glioblastoma cells line: U-87 MG cells.

2. Materials and methods

2.1. Materials

PLGA (50:50 wt%, MW 30000 g mol⁻¹) pellets were obtained from Shenzhen Esun Industrial Co., China. Polyvinyl alcohol (PVA), fully hydrolyzed (MW 30000 g mol⁻¹), was bought from Merck (Germany). MTX (purity > 97%) was bought from the Excella GmbH company (Germany). PTX, acetone (> 99.9%), fetal bovine serum (FBS), trypsin, phosphate-buffered saline (PBS) and penicillin/streptomycin were bought from Sigma-Aldrich (Germany). The U-87 MG (human glioblastoma) and B65 (rat neuroblastoma) cell lines were purchased from the cell bank of Pasteur Institute (Iran). Annexin V/propidium iodide was obtained from BioLegend. A lactate dehydrogenase kit, Sigma-Aldrich (Cat #: TOX7) and Bcl-2 antibody was purchased from Abcam (ab32124).

2.2. Preparation of nanoparticles

Nanoparticles were prepared by a nanoprecipitation method [7] with two surface modifications using PVA and a combination of PVA

and P188. Briefly, 50 mg of PLGA was dissolved thoroughly in 10 mL of acetone using magnetic stirring at room temperature. Afterwards, 2.5 mg of MTX and 2.5 mg PTX were added to this polymeric solution followed by the addition of 100 mL aqueous solution of PVA. Another group of nanoparticles was prepared using both PVA (90 mL 1% W/V) and P188 (10 mL, 1% W/V) as stabilizers. The prepared solution was left overnight under magnetic stirring at room temperature to evaporate the acetone. At last, nanoparticles were collected through centrifugation at 12000 rpm for 30 min and the pellets were washed twice with distilled water in order to remove the non-encapsulated drugs. Finally, the nanoparticles were suspended in sucrose (2% w/v) and freeze-dried (Telstar, IyoQuest).

2.3. Characterization of nanoparticles

2.3.1. Particle size analysis and zeta potential measurements

The mean particle size and size distribution of the nanoparticles were assessed through the dynamic light scattering (DLS) method using a nanoparticle size analyzer (scatterscope1, K-ONE, S. Korea). The Zeta potential of suspended particles was also determined by electrophoretic laser Doppler anemometry using a zeta potential analyzer (Malvern Zetasizer ZEN 3600).

2.3.2. Morphological assessment of nanoparticles

The morphology of the nanoparticles was determined by a scanning electron microscope (SEM). Nanoparticles were dried on aluminum foil. Each sample was sputter-coated with gold/palladium for 120 s at 14 mA under an argon atmosphere for secondary electron emissive SEM and the particle morphology was observed at an acceleration voltage of 15 kV.

2.3.3. Determination of EE% and DL%

Standard curves of PTX and MTX were obtained in acetone and PBS separately. Briefly, different concentrations of PTX (5–100 ppm) and MTX (2–60 ppm) were prepared. UV-visible (Cecil CE 7250, England) absorption of each sample was measured at 228 nm (PTX) and 373 nm (MTX). The standard curve was considered as the absorbance versus concentration (R², linearity). All experiments were performed in triplicate. The EE [13,14] and DL [13] were calculated using the equations below:

$$EE\% = \frac{\text{amount of drug applied for nanoparticle preparation (mg)} - \text{amount of drug in the supernatant (mg)}}{\text{amount of drug applied for nanoparticle preparation (mg)}} \times 100$$

$$DL\% = \frac{\text{amount of drug applied for nanoparticle preparation (mg)} - \text{amount of drug in the supernatant (mg)}}{\text{amount of dried nanoparticles (mg)}} \times 100$$

2.3.4. DTA and TGA

DTA and TGA were used to investigate the thermal behavior of the samples. The analysis was performed on MTX, PTX, NP1 and Co-1 NPs formulations using a thermo analyzer (model STA 503, Germany). Briefly, approximately 10 mg of each sample was placed on open pans of aluminum oxide and analyzed between room temperature and 1000 °C at the rate of 10 °C min⁻¹. At the end, the weight loss and differential temperature were recorded and plotted against temperature.

2.4. In vitro release study

The drug release from each sample was performed in PBS containing dimethyl sulfoxide (DMSO) at a ratio of 1:10. Samples were poured in a dialysis bag and were placed in a shaking incubator at 37 °C and 100 rpm (Labtech, S. Korea). Samples from the release media were

collected at pre-determined time intervals (0.5, 1, 2, 3, 6, 12, 24, 48, 72 and 120 h) under the sink condition and optical absorbance were measured through UV-visible spectroscopy at 228 nm and 373 nm for PTX and MTX, respectively. The release profile of each sample with respect to time was also statistically analyzed through a one-sample T and Wilcoxon Test and the statistical test for the release of various samples at the same time points was accomplished by one-way ANOVA.

2.5. Hemolysis test

Healthy volunteer blood specimens were collected in BD vacutainer tubes containing sodium citrate (3.8% wt) at a ratio of 9:1 for anticoagulation. Then, the blood at a ratio of 1:50 was diluted with PBS and was kept for 30 min at 37 °C. Co-1 NPs, Co-2 NPs and PLGA NP1 samples were redispersed in PBS and then the samples were incubated with 0.2 mL of diluted blood for 3 h. Centrifugation was performed for 5 min at 1500 rpm to separate the supernatant. DMSO and PBS were used as positive and negative controls, respectively. The optical density (OD) of each sample at concentrations of 0.025–1.5 mg·mL⁻¹ was read by a plate reader at a wavelength of 545 nm (Nanodrop Plate Reader, Seoul, South Korea).

2.6. In vitro cellular uptake study

Fluorescent nanoparticles were prepared by loading Rhodamine B into NP2. U-87 MG cells (at a density of 1 × 10⁵ cells per well) were placed in a 24-well culture plate and were incubated for 12 h at 37 °C in a 95% CO₂ humidified incubator. After 12 h, the Co-NPs were added for 2 h. Then, the cells were washed with PBS. The cellular nuclei were stained with 4',6-diamidino-2-phenylindole (DAPI). Cells were observed using a fluorescence microscopy (Olympus BX43) to investigate the uptake level of the PLGA NPs loaded with Rhodamine B coated with PVA/P188.

2.7. MTT assay

The cytotoxicity of the drug-loaded nanoparticles was assessed using MTT (3-(4,5-dimethylthiazol-2-yl)-2,5-diphenyltetrazolium bromide) assays. U-87 MG and B65 cell lines (at a density of 1000 cells per well) were seeded in a 96-well culture plate and were incubated for 12 h in order to allow the cells to attach to the culture plate. The cells were then treated with NP2, MTX, PTX, mix free, PTX NP2, MTX NP2, mix NPs, Co-1 and Co-2 NPs at various concentrations of 1, 5, 12.5, 25, 50, 100 and 200 µg·mL⁻¹ for 24, 48 and 72 h. 100 µl of DMEM containing MTT (0.5 µg·mL⁻¹) was added to each well and incubated at 37 °C for 4 h. The MTT solution was removed and 100 µl of DMSO was added in order to dissolve the formazan crystals. The absorbance was measured at 570 nm using a microplate reader [15–17].

2.8. LDH assay

Similar to the group distribution mentioned in the MTT assay section at their IC₅₀ concentrations, 50 µl of a mixture (LDH Assay Buffer and LDH Substrate Mix) was added to each well containing cells and was incubated at 37 °C for 30 min. The absorbance of LDH expression was assessed at 450 nm using a microplate reader. Triton X-100 (1%) in PBS (pH 7.4) was used as a positive control.

2.9. Early detection of apoptosis by Annexin-V

The evaluation of cell death after the treatment of U-87 MG cells with the above-mentioned formulations (PTX NP2, MTX NP2, MTX, PTX, a mix free, mix NPs, Co-1 NPs and Co-2 NPs) was performed by staining the cells with an Annexin V-FITC and a propidium iodide solution followed by flow cytometry analysis. Briefly, U-87 MG glioma cells were seeded at a density of 1 × 10⁶ cells per well in a 6-well

culture plate and were allowed to adhere. After 24 h, the cells were exposed to all formulations at the IC₅₀ value for each drug (as obtained in the MTT assay) and PLGA NPs were used as the control. After incubation for 48 h, the cells were harvested and centrifuged at 2000 rpm for 5 min, and then were washed twice with PBS. The pellet was then re-suspended in 400 µl PBS and 100 µl of a buffer containing Annexin and propidium iodide. Finally, the stained cells (with Annexin V-FITC and propidium iodide) were evaluated by flow cytometry. The Quadrant gate for each sample was set by its negative control (unstained sample).

2.10. Bcl-2 pathway analysis

Bcl-2 is considered as an apoptotic index due to its anti-apoptosis effect [18]. The expression level of this protein was evaluated through immunofluorescence. Cells were exposed to free drugs and various formulations of the drug including PTX NP2, MTX NP2, MTX, PTX, mix free, a mix of NPs, Co-1 NPs and Co-2 NPs. Then, the cells were left in serum-free medium overnight on glass cover slips. Afterwards, the U-87 MG cells were fixed in 4% paraformaldehyde in PBS for 10 min and washed twice with PBS. The cells were then permeabilized with 0.25% Triton X-100 in PBS for 5 min and incubated in PBS containing 5% bovine serum albumin for 1 h to prevent non-specific binding. The cells were then incubated with an anti-Bcl-2 antibody overnight at 4 °C and Alexa Fluor 488-conjugated goat anti-rabbit IgG detected. The cells were stained with 4',6-diamidino-2-phenylindole (DAPI) to visualize the cell nuclei under an Olympus FluoView™ 1000 confocal microscope.

2.11. Statistical analysis

All data are represented as the mean ± standard deviation (SD) and the p value < 0.05 was considered statistically significant via GraphPad Prism, version 8.3.0 software. One way-ANOVA tests or t-tests were carried out for each statistical analysis.

3. Results

3.1. Physicochemical characterization of NPs

The physicochemical properties of the NPs are summarized in Table 1. It can be observed that all NPs had a mean particle size

Table 1
Physicochemical characteristics of nanoparticles including size, zeta potential, encapsulation efficiency and drug loading.

Nanoparticle	Mean diameter (nm) ± SD	PDI	Zeta potential (mV) ± SD	EE (%)	DL (%)
NP	50 ± 6	0.12	-24.6 ± 0.31	-	-
NP1	65 ± 3	0.04	-8.02 ± 0.24	-	-
NP2	84 ± 7	0.08	-14.2 ± 0.18	-	-
MTX NP1	100 ± 3	0.03	-7.93 ± 0.15	69	9.8
MTX NP2	109 ± 5	0.04	-13.02 ± 0.19	75	12
PTX NP1	223 ± 6	0.02	-7.2 ± 0.10	92	8.5
PTX NP2	241 ± 19	0.07	-10.58 ± 0.34	89	8.4
Co-1 NPs	180 ± 8	0.04	-8.59 ± 0.20	MTX: 70 PTX: 88	MTX: 4 PTX: 5
Co-2 NPs	212 ± 16	0.07	-15.7 ± 0.16	MTX: 72 PTX: 85	MTX: 4 PTX: 4.9

NP: PLGA nanoparticles without any coating.

NP1: PLGA nanoparticle coated with PVA.

NP2: PLGA nanoparticles coated with PVA/P188.

MTX NP1: MTX loaded PLGA nanoparticles coated with PVA.

MTX NP2: MTX loaded PLGA nanoparticles coated with PVA/P188.

PTX NP1: PTX loaded PLGA nanoparticles coated with PVA.

PTX NP2: PTX loaded PLGA nanoparticles coated with PVA/P188.

Co-1 NPs: MTX/PTX co-loaded PLGA nanoparticles coated with PVA.

Co-2 NPs: MTX/PTX co-loaded PLGA nanoparticles coated with PVA/P188.

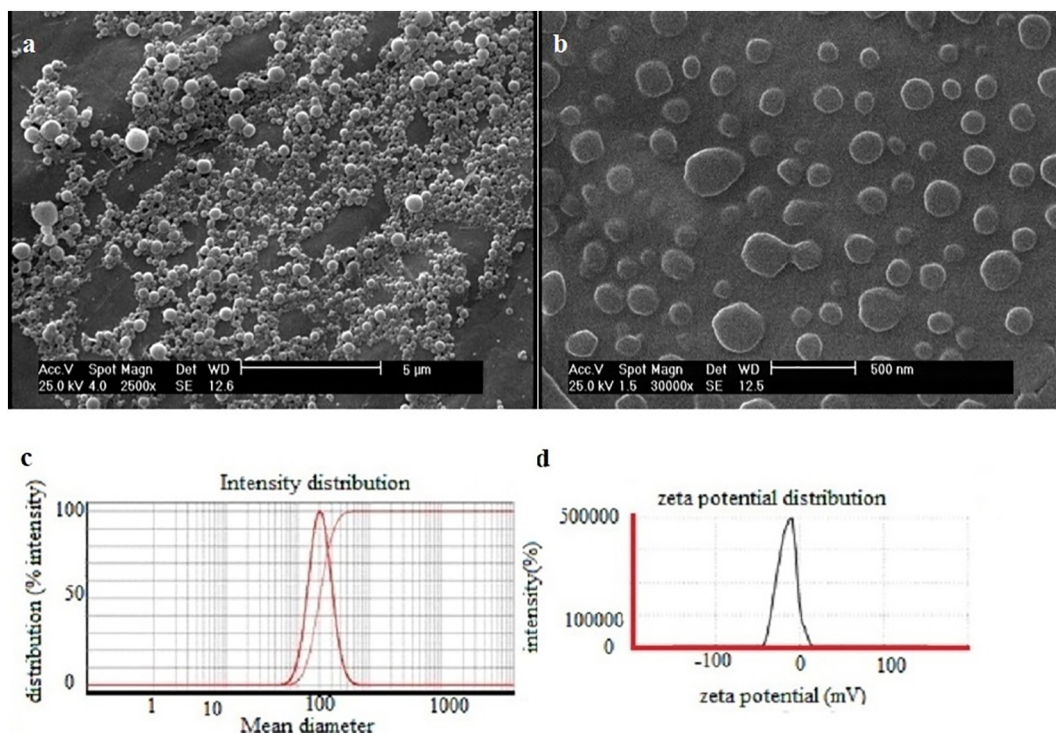


Fig. 1. SEM image a) before dilution, b) after dilution, c) DLS and d) zeta potential of Co-2 NPs.

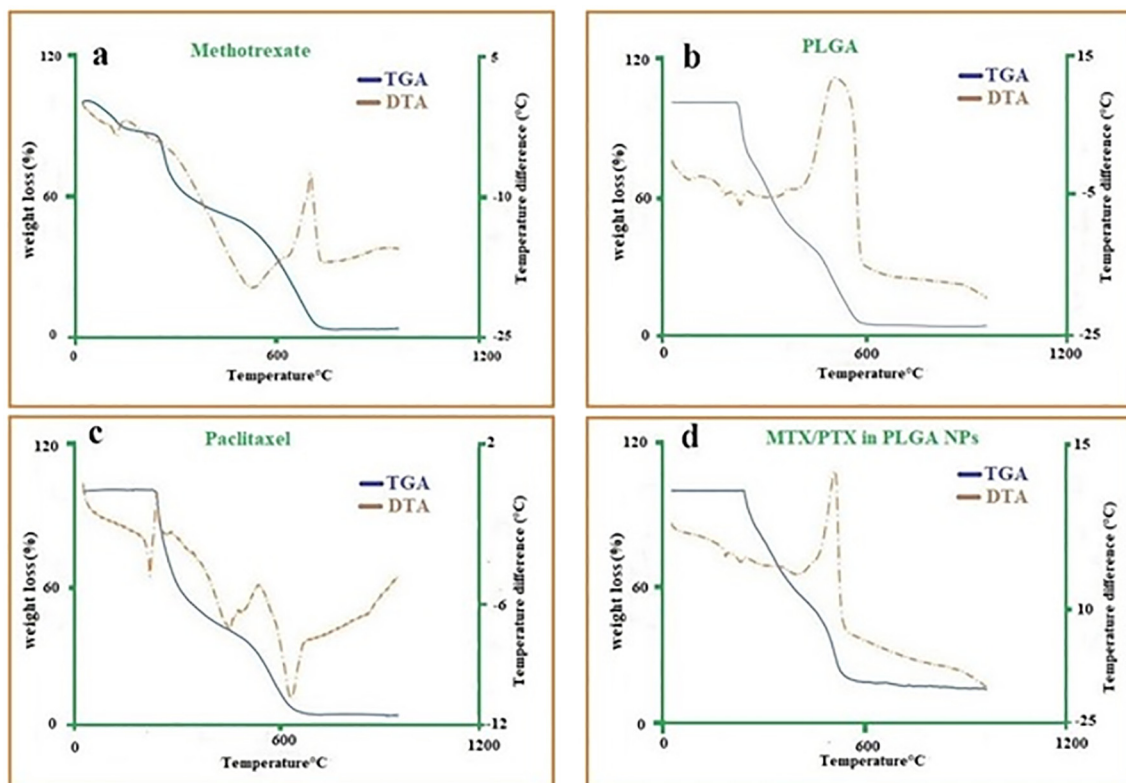


Fig. 2. DTA (solid line) and TGA (broken line) thermographs: a) MTX, b) PLGA, c) PTX and d) Co-1 NPs.

between 50 and 230 nm as measured by DLS. The mean diameter of the PLGA NPs prepared without any stabilizer was about 50 nm which increased to 65 nm and 80 nm upon the addition of PVA and PVA/P188 to the preparation process, respectively. It was observed that the mean diameter of MTX NP2 and PTX NP2 increased by the addition of P188.

Co-2 NPs had a mean diameter of about 200 nm. SEM images showed that the Co-2 NPs shape was spherical with a smooth surface (Fig. 1a and b). The DLS results demonstrated that the Co-2 NPs had diameters from 50 nm to 800 nm with a PDI of 0.07 (Fig. 1c). The zeta potential for all NPs ranged from -7.2 ± 0.10 mV to -24.6 ± 0.31 mV

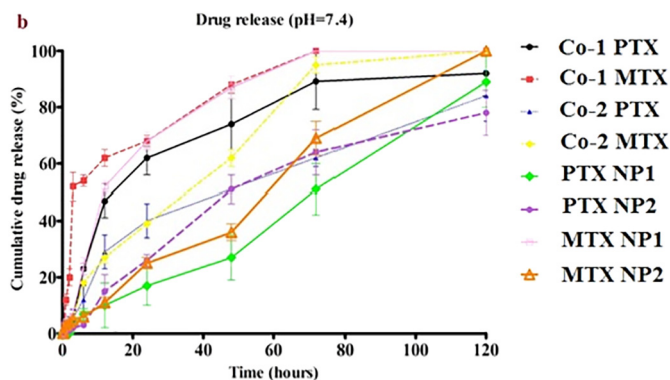


Fig. 3. In vitro release profile of NPs in PBS medium (pH 7.4).

Co-1 PTX: release of PTX from Co-1 NPs.

Co-1 MTX: release of MTX from Co-1 NPs.

Co-2 PTX: release of PTX from Co-2 NPs.

Co-2 MTX: release of MTX from Co-2 NPs.

PTX NP1: release of PTX from PTX NP1.

PTX NP2: release of PTX from PTX NP2.

MTX NP1: release of MTX from MTX NP1.

MTX NP2: release of MTX from MTX NP2.

(Table 1). Fig. 1d shows the zeta potential of the Co-2 NPs with a single peak at -15 mV. In all samples with or without drugs, the zeta potential became more negative upon the addition of P188. For instance, the zeta potential of Co-1 NPs was -8.59 ± 0.02 mV, which reached -15.7 ± 0.16 mV by the addition of P188.

3.2. EE% and DL%

The EE% was about 69% to 92% and the range of the drug loading was about 4% to 12% for all of the prepared NPs. The EE% for MTX and PTX in the Co-2 was 72% and 85%, and the DL% was about 4% and 4.9%, respectively (Table 1).

Analysis of the MTX free drug (Fig. 2a) revealed three TGA steps and three broad DTA peaks. The first TGA step was the result of an endothermic reaction, which was around 100 °C. The other steps were between 130 °C, 246 °C, 336 °C and 505 °C. DTA peaks on the other hand were located at 117 °C, 230 °C and 522 °C. The three step decomposition of MTX in the TGA curve was due to the trihydrate form of the drug [19]. The peaks at 117 °C and 230 °C on the DTA curve are in agreement with those observed by de Oliveira et al. at 122 °C and 231 °C, respectively. The authors argued that the first peak at 117 °C corresponds to dehydration whilst the second one at 230 °C was because of crystalline MTX melting [20]. PLGA had a single step weight loss between 212 °C and 600 °C and a sharp peak at 190 °C in DTA (Fig. 2b). Several broad peaks were detected in DTA at 225 °C, 308 °C and 489 °C for the PLGA NPs. PLGA NPs exhibited relative thermal stability until they reached a temperature of 209 °C. Thereafter, the NPs experienced a 90% weight loss as a result of thermal decomposition. Only 4% of the residual mass of the blank PLGA NPs was left after 600 °C. Such findings correlate well with similar data in the literature [21,22]. For example, Silva et al. reported a thermal decomposition at 205 °C with $> 90\%$ of weight loss near 600 °C [21]. The sharp peak at 180 °C measured by DTA represents the thermal decomposition of sucrose, whilst other peaks at 225 °C and 308 °C are the result of PLGA decomposition. The thermal decomposition of the PTX drug revealed that PTX can be thermally stable up to 240 °C in TGA (Fig. 2c). A further

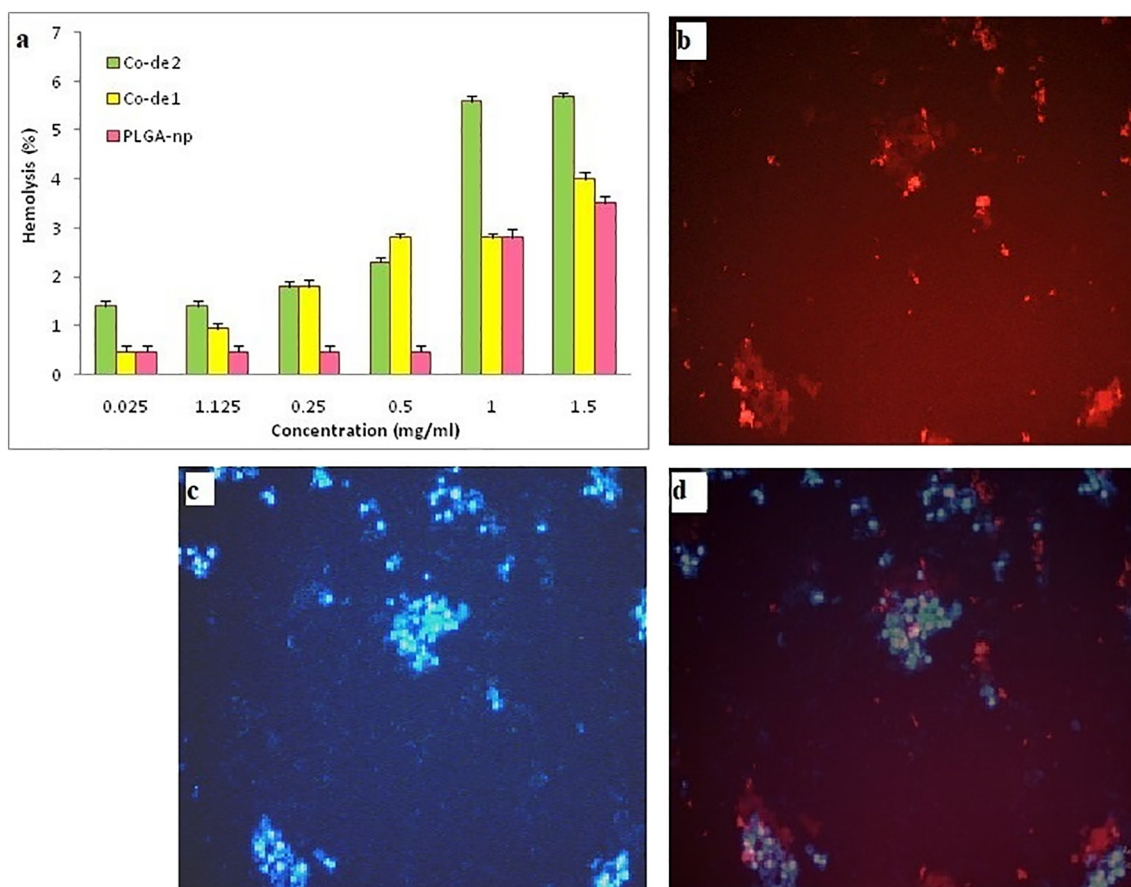


Fig. 4. a) Hemolysis assays of NP1, Co-1 NPs, and Co-2 NPs. Uptake of b) Rhodamine B loaded PLGA NPs, c) DAPI staining and d) overlayed pictures (magnification $20\times$).

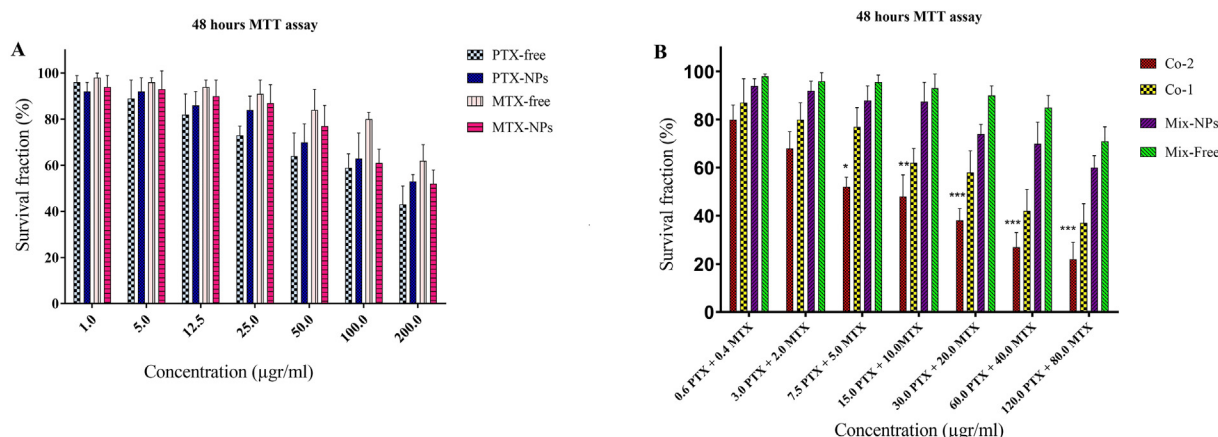


Fig. 5. MTT results after 48 h of incubation in the U-87 MG cells. Data represent mean ± SD (n = 3). * indicated p < 0.05, ** indicated p < 0.01, *** indicated p < 0.001 and (compared to the control group).

Table 2

The IC₅₀ values of cells after 48 h of treatment with different groups of nanoparticles and free drugs.

IC ₅₀ values (µg·ml ⁻¹)	PTX free	PTX NPs	MTX free	MTX NPs	Co-2		Co-1		Mix NPs		Mix free	
					PTX	MTX	PTX	MTX	PTX	MTX	PTX	MTX
U-87 MG	49.0	61.0	669.0	68.5	24.5	9.5	39.2	18	56	30	274	195.5
B65	16	6.7	132	6.7	13.41	5	26.82	15.81	15.16	6.66	17.66	9.03

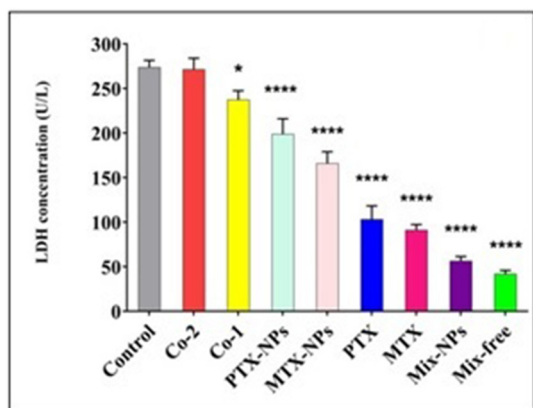


Fig. 6. LDH assay graph. Data represent mean ± SD (n = 3). * indicated p < 0.05, and **** indicated p < 0.0001 (compared to the Control group).

increase in temperature revealed another state of the drug. Specifically, the crystalline form of PTX exhibited a sharp peak in DTA at 221 °C, which indicates the drug's thermal transition in TGA. Another small kink was observed at 340 °C with a sharp peak at 453 °C, consistent with TGA results. These results are in good agreement with those obtained by Hiremath et al. [23]. The analysis of the Co-1 NPs thermograms (Fig. 2d) showed a single step TGA curve with an onset at about 240 °C. DTA curves on the other hand showed peaks at 182 °C, 220 °C and a broad peak centered at 388 °C. From these results, the single step nature of the TGA is analogous to both PLGA and PTX curves. It can be postulated that the extension of the peak to 240 °C is a result of the thermal stability of PTX in the formulation. It is noted that the weight loss of MTX/PTX PLGA NPs are less than PTX, MTX, and PLGA which may be attributed to PVA and P188 coated on the MTX/PTX PLGA NPs. Furthermore, the DTA peak at 182 °C can be ascribed to PLGA whilst the peak at 220 °C can be attributed to MTX. Therefore, we can conclude that whilst MTX existed in its crystalline form within the vehicle [20], PTX only existed in its amorphous form [23].

3.3. In vitro drug release

NPs control drug release to increase drug bioavailability and decrease drug toxicity throughout the body. The in vitro release profile of MTX and PTX demonstrated a time and pH-dependency. Results indicated that the drug release from the PLGA NPs was much faster in an acidic environment pH (6.5) compared to a neutral pH (7.4) medium. An acidic pH increases the hydrolyzation of ester linkages in PLGA and helps to release encapsulated drugs in a controlled and sustained manner. At first, an initial burst release was observed followed by a gradually slow and continuous release which was similar at both pH 6.5 (Fig. S1) and 7.4 (Fig. 3). However, the release trend became slower by the modification of P188 on the NPs' surface. The release profile of PTX extended more from the Co-2 NPs compared to the Co-1 NPs. In addition, long-lasting drug release was observed for the Co-2 NPs compared to the Co-1 NPs, indicating the protective effect of the coating with P188 on the NPs (Fig. 3). It is noted that the release profile of each sample with respect to time was also statistically analyzed through a one-sample T and Wilcoxon Test and the statistical test for the release of various samples at the same time points was accomplished by one-way ANOVA. The statistical analysis of each sample is demonstrated in Table S1.

3.4. Hemolysis test

The hemolysis results from the Co-1 NPs and Co-2 NPs are depicted in Fig. 4a. The hemolysis rate for all the samples at low concentrations (0.025, 0.125, 0.25 and 0.5 mg·mL⁻¹) were < 5% after incubation for 180 min, indicating that the samples were non-hemolytic. In contrast, the hemolysis rate at higher concentrations (0.5 and 1 mg·mL⁻¹) were > 5%, therefore, these concentrations did not follow ISO 10993-4:2002. In summary, Co-2 NPs showed a higher hemolysis rate than Co-1 NPs and other NPs for all concentrations.

3.5. Cellular uptake study

The efficiency of cellular uptake was assessed by an inverted

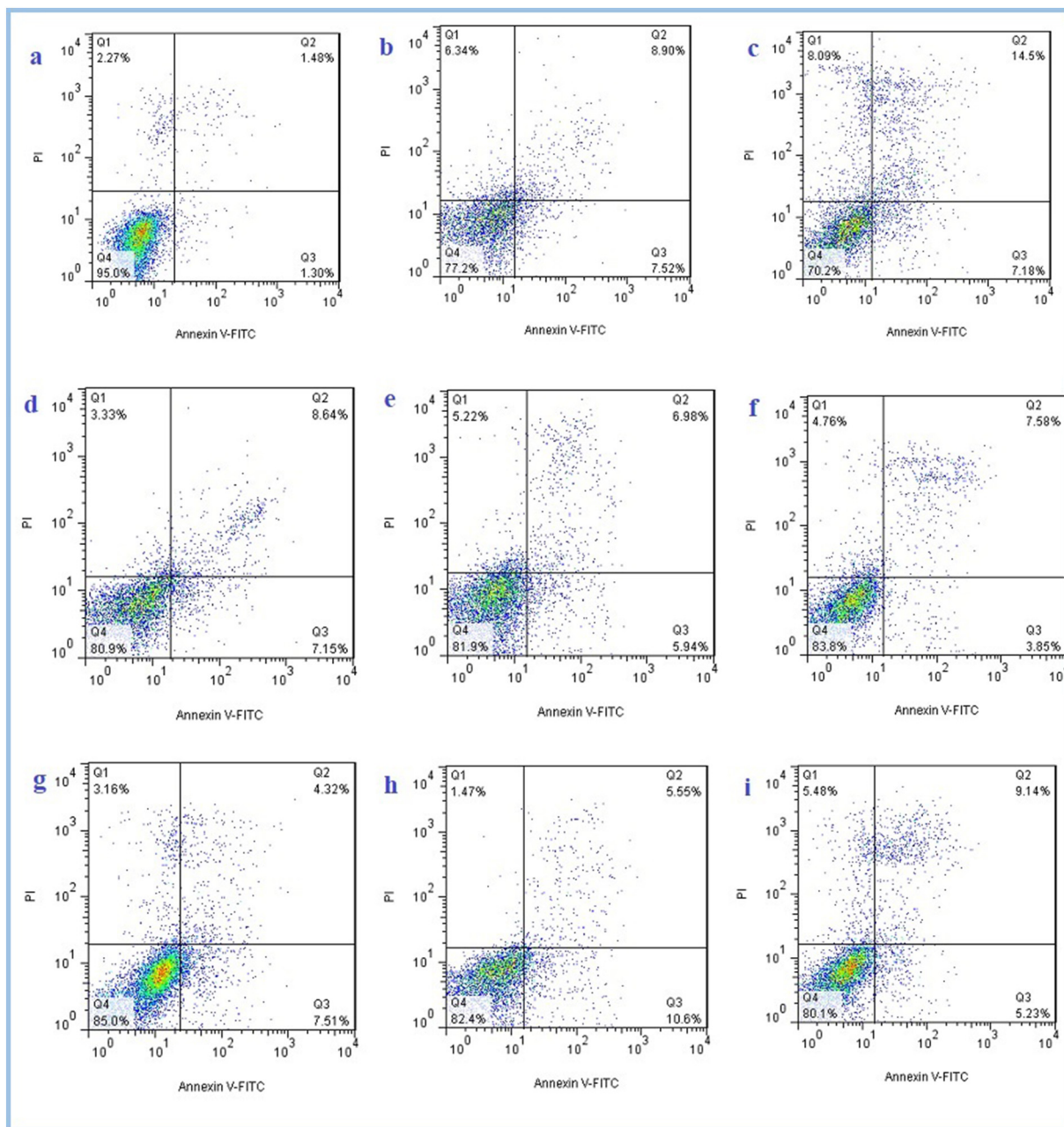


Fig. 7. Flow cytometry assay of the a) control (without any treatment), b) Co-1 NPs, c) Co-2 NPs, d) PTX NP2, e) mix of NPs, f) PTX, g) MTX, h) MTX NP2, and i) mix free on the U87 MG cell line. (The Quadrant gate for each sample was set by its negative control (unstained sample).)

fluorescence microscope. After incubation for 2 h, red fluorescence signals were observed in the cytoplasm suggesting that this nanocarrier could deliver the drug into U-87 MG cells (Fig. 4b, c and d).

3.6. MTT assay

Here, two chemotherapeutic drugs (MTX and PTX) were loaded into the same carrier in order to assess the efficiency of a co-delivery system into U-87 MG cells. The cytotoxicity effect of PTX NP2 and MTX NP2 were compared with free PTX and free MTX, respectively. Applied concentrations ranged between 1 and 200 $\mu\text{g}\cdot\text{mL}^{-1}$ with an incubation time of 48 h (Fig. 5A). The results indicated that the survival rate of the cells was concentration dependent. As shown in Fig. 5B, Co-2 NPs decreased cell viability compared to other comparable groups containing Co-1 NPs, a mix of free, and a mix of NPs. Table 2 shows the IC_{50} values of all samples after 48 h of treatment. It was observed that free PTX was

more cytotoxic than PTX NP2 after 48 h. In contrast, the survival rate of cells treated with MTX NPs was lower than MTX free for all applied concentrations after incubation for 48 h. The cytotoxicity of the various formulations on B65 cells is shown in Fig. S2. It was observed that like the U-87 MG cells, B65 cells were more sensitive to Co-2 NPs than all other groups after incubation for 48 h. According to Table 2, the IC_{50} values for Co-2 NPs were 24.5 $\mu\text{g}\cdot\text{mL}^{-1}$ and 9.5 $\mu\text{g}\cdot\text{mL}^{-1}$ for PTX and MTX, respectively. In addition, as seen in Table 2, Free PTX had more of a therapeutic effect on U-87 MG cells than the combination of free MTX and PTX. This may be related to the inadequate penetration of PTX due to the combination with free MTX. However, Co-2 NPs had a better therapeutic effect than MTX NPs or PTX NPs on U-87 MG cells. The reason may be related to co-delivery which is considered as a promising strategy for combined anticancer drugs to increase therapeutic effects due to the simultaneously entrance of drugs to cancer cells whereas MTX NP2 and PTX NP2 have different sizes which affect their entrance,

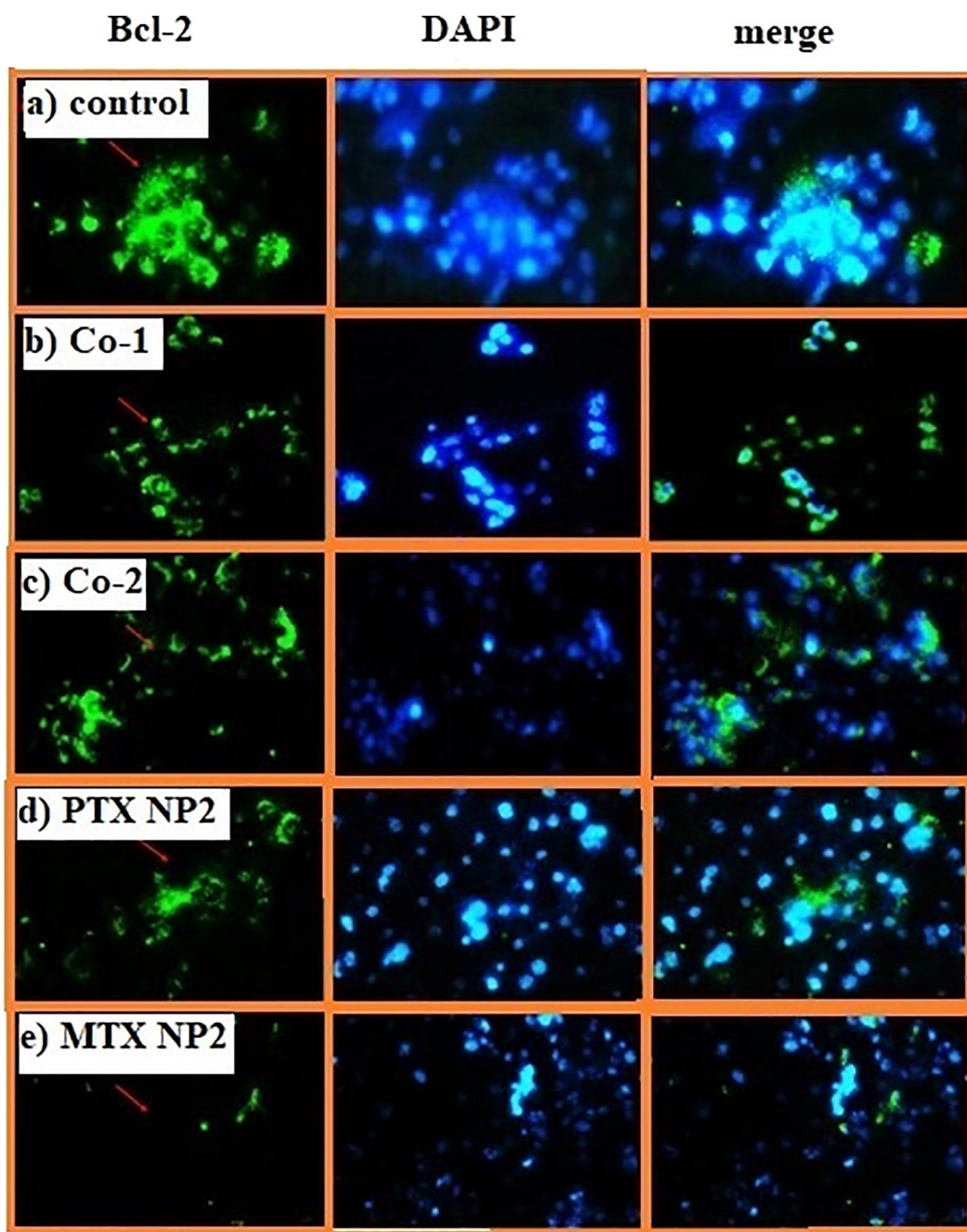


Fig. 8. Bcl-2 expression in the U87 MG cell line treated with NPs. a) control, b) Co-1 NPs, c) Co-2 NPs, d) PTX NP2, and e) MTX NP2 (magnification $400\times$).

leading to decrease in synergistic/additive effect.

3.7. LDH assay

LDH is a cytosolic enzyme used as a tool to test cell membrane integrity and necrosis. This enzyme is released from damaged cell membranes. The amount of released LDH was higher in the U-87 MG cells when exposed to the co-delivered NPs for both Co-1 NPs and Co-2 NPs than the other groups (Fig. 6). The highest released LDH was seen for the Co-2 NPs, which was about $271.5 \text{ U}\cdot\text{L}^{-1}$. The release of the LDH enzyme was more for the PTX NP2 and MTX NP2 compared to the free drugs. The lowest amount was for the combination of free drugs.

3.8. Apoptosis induced by nanoparticles

Apoptotic and necrotic cell death were investigated by the Annexin V-FITC/PI test and the results are presented in Fig. 7. All cells (viable and dead) were distributed into four sections, namely Q1, Q2, Q3 and Q4. Cells which are in the Q4 section are unstained, i.e., they are Annexin negative and propidium iodide negative (Ann^-/PI^-) and, thus, are viable. The Q3 section contains cells which are Ann^+/PI^- , meaning that they are in early apoptosis. In the Q2 section, there are cells, which are both Ann^+ and PI^+ , implying last stage apoptosis whilst the Q1 section contains cells with Ann^-/PI^+ character, demonstrating that they are necrotic. The highest amount of necrosis (Q1) was observed when the U-87 MG cells were exposed to the Co-1 and Co-2 NPs. Cells treated with the Co-2 NPs demonstrated 21.68% and 8.09% apoptosis and necrosis, respectively; apoptosis was 16.42% and necrosis was

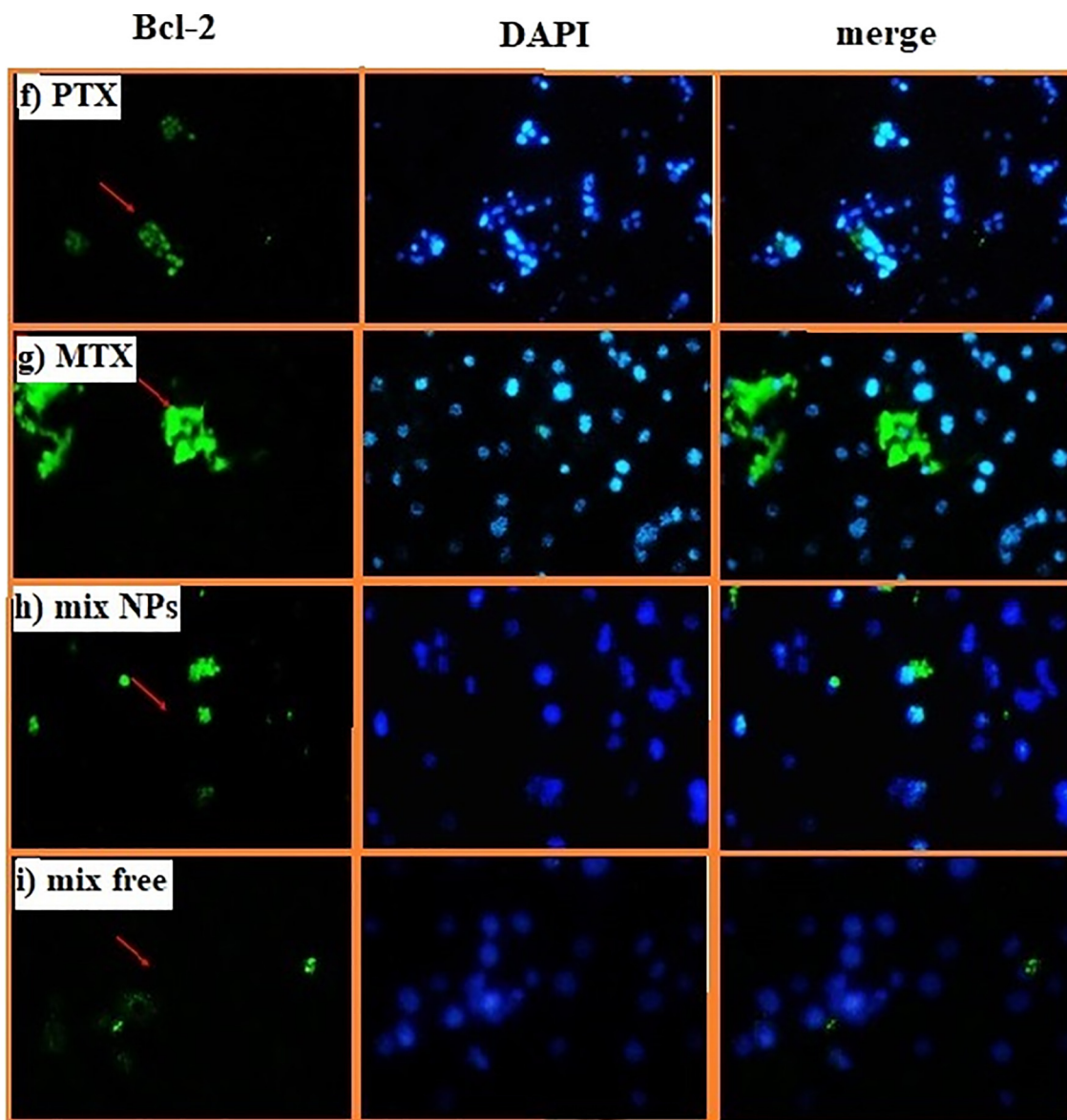


Fig. 9. Bcl-2 expression on U87 MG cell line treated with NPs. Raw f) PTX, g) MTX, h) mix of NPs, and i) mix free (magnification 400 \times).

6.34% for the Co-1 NPs treatment. Free MTX and free PTX induced higher amounts of necrosis (3.16% and 4.76%) than MTX NP2 (1.47%) and PTX NP2 (3.33%), respectively.

3.9. Bcl-2 analysis

To evaluate the effect of the encapsulated drugs on apoptosis, DAPI staining of DNA and Bcl-2 protein expression were performed. As shown in Figs. 8 and 9, smooth and homogenous nuclei were observed for the DAPI staining and Bcl-2 protein expression for the immune fluorescence, which is the reason that the cells seem to be alive. However, for the treatment groups with the various formulations (PTX NP2, MTX NP2, MTX, PTX, mix NPs, mix free, Co-1 NPs, and Co-2 NPs), the nuclei morphology was segmented and fragmented and Bcl-2 protein expression decreased where the DAPI overlay appeared to be small. According to the results of this assay, the trend for the amounts of DAPI and Bcl-2 expression overly was: positive control > Co-2 NP > Co-1 NP > PTX NP2 > free MTX > MTX NP2 > free PTX > mix NPs > mix free, respectively (Figs. 8, 9 and S3). Therefore, the most apoptosis via the Bcl-2 pathway was seen for the free drugs and the mix of NPs. Moreover, a change in the nuclei morphology was seen for all the samples in

contrast with the negative control.

4. Discussion

PTX and MTX are two chemotherapeutic agents used to treat various cancers. Having said that, their administration is limited owing to the side effects they create in the body. This study aimed to load PTX and MTX in PLGA NPs covered with P188 to enhance drug delivery efficiency and reduce side effects. As stated earlier, nanocarriers play an important role in successful drug transport through the BBB [24] to reduce drug toxicity to normal tissues by minimizing a large amount of drug release [25,26]. It is believed that only NPs coated with surfactants (such as tween 80 and poloxamers like pluronic® F-68) are able to transfer across the BBB. One of the claimed mechanisms for this phenomenon is receptor-mediated endothelial cell endocytosis. This phenomenon is described by ApoB, ApoE and ApoA-1 absorbance from blood to the NP surface. Therefore, it has been widely speculated that NPs coated with the mentioned surfactants cross the BBB by apolipoprotein adsorption [27]. Fig. 10 is a schematic of this phenomenon. However, another mechanism for NP BBB crossing is via a P188 coating where P188 solubilizes the cell membrane as a surfactant and

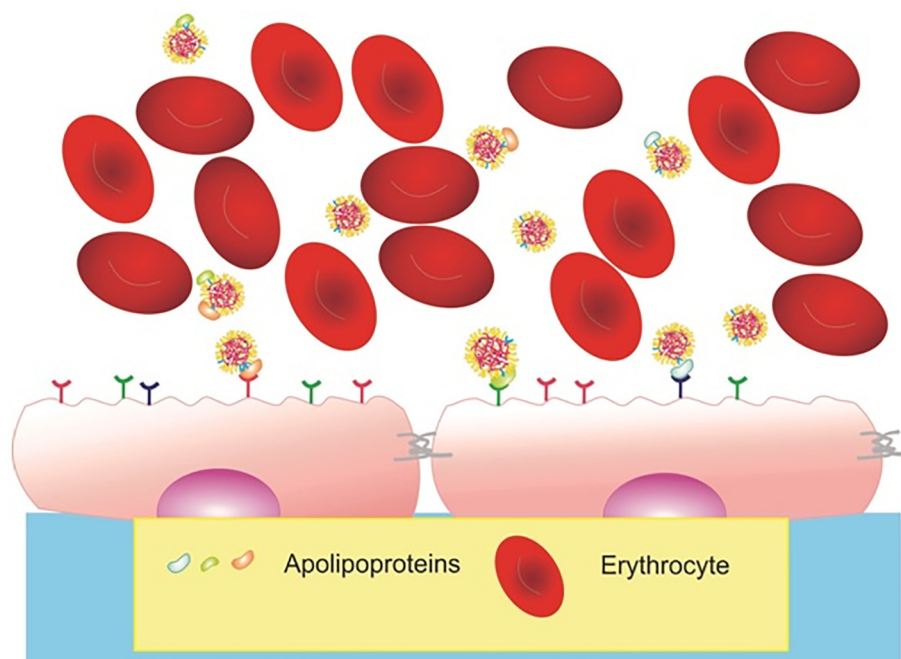


Fig. 10. Schematic view of apolipoprotein adsorption on P188 coated NPs.

afterwards the NPs can easily enter cells [28]. Another unique property of poloxamers is their resistance against the multidrug resistance (MDR) effect which constitutes a major challenge in cancer treatment [29]. In our study, the cellular uptake of Rhodamine B labeled NP2 was evaluated using U-87 MG cells in order to confirm the role of P188 in cellular penetration, and DAPI was used for cellular nuclei staining.

This study focused on a co-drug delivery system able to transfer two drugs toward cancer cells simultaneously. The selection of a suitable technique for the preparation of this kind of NP with various water solubility properties is important in such systems. Different studies have reported that the co-precipitation method is highly efficient in order to provide co-delivery. Hence, a co-precipitation method was used here for the preparation of co-loaded PLGA NPs [30,31]. In the present study, PVA was used as a stabilizer to produce stable NPs of a suitable size (150–250 nm) and such NPs were further coated with P188 due to the reasons mentioned above [32]. The mean diameter of NPs increased when we applied P188 to the NPs. Moreover, the mean zeta potential decreased upon the addition of P188. In another study, PLGA NPs containing docetaxel were prepared by using different solvents. It was observed that NPs with P188 on their surface possessed larger mean diameters compared to NPs without P188 using dichloromethane as a solvent. The mean diameter of the NPs increased from 265 nm to 290 nm after a P188 coating and the zeta potential decreased from -16.06 mV to -19.27 mV when using chloroform as an organic solvent. In the preparation of the NPs by ethyl acetate, their mean diameter and mean zeta potential changed from 398 nm to 438 nm and from -19.2 nm to -20.75 nm, respectively, when using a P188 coating [28]. Different studies have reported that controlling drug release is one of the most important properties of a nanocarrier system for cancer treatment. It has been observed that a drug is usually released faster in an acidic environment (pH 6.5) [33] than a neutral one (pH 7.5) [34]. One reason for this faster release is the degradation of a polymer carrier and reduction of the ionic interactions between the drug and polymer at low pH [35]. PLGA is exposed to autocatalytic acidic degradation as it is an ester based polymer. However, drug release is slow and controlled in coated NPs compared to uncoated NPs at pH 6.5 and 7.4, which can be attributed to the coating protecting the NP [35].

Here, we observed that MTX released slower and with fewer burst

release from the MTX NP2 compared to MTX NP1. This can be attributed to the characteristics of P188 which creates a more hydrophilic and acceptable medium for MTX in the NPs. Moreover, the release profile of PTX was longer and had less burst release from the Co-2 NPs compared to Co-1 NPs at pH 7.4. Here, it is suggested that MTX is located on the outer area of the NPs because of the existence of P188 and the pharmacological features of MTX. We suggest that PTX is located in the inner spaces of the NP so that most of the PTX will be released to the media when the NP degrades. Therefore, a slower release of PTX by the P188 coating will result.

It has been reported that the EE of docetaxel increased in the presence of P188 compared to a PVA only coating, and the drug release profile possessed a weaker burst release which was sustained in the presence of P188 [28]. Further, PLGA can produce minimal systemic toxicity when hydrolyzed into two endogenous and natural metabolites, such as lactic acid and glycolic acid in the body [36–38]. The combination of two drugs in the NP is an effective approach to decrease systemic toxicity and the side effects of drugs [39,40]. PTX and MTX are chemotherapeutic drugs with distinct solubility properties and different anticancer functions for brain tumors [31,41]. Here, PTX and MTX were loaded into a carrier to enhance a chemotherapeutic effect. Significant reduction was observed in the survival rates of U-87 MG cells. Such NPs may enter cells through endocytosis or phagocytosis in order to induce a cytotoxic effect [42] where MTX can inhibit DNA synthesis and stimulate a series of intracellular signaling events inducing apoptosis in U-87 MG cells. Furthermore, PTX can stop microtubule assembly and disrupt microtubule networks in a cell, thereby causing cell apoptosis [43].

Several successful combinations of chemotherapeutics (especially MTX with PTX) have been reported. For example, the combinations of PTX, MTX and cisplatin have been successful for treating urothelial malignancies [44]. Further, a synergistic effect of tiazofurin, PTX and MTX for cancer has been suggested [45]. Moreover, the combinations of MTX, PTX and doxorubicin have been a strong strategy against human breast cancer cells [46]. According to our results, a co-drug delivery formulation demonstrated more cytotoxicity than nanoparticles loaded with just one drug (MTX or PTX) and free drugs. In addition, Co-2 NPs were more cytotoxic than Co-1 NPs which can be attributed to the presence of P188 on the surface of the NPs. This result could be

attributed to the sustained release of drugs from P188 coated NPs and better penetration of Co-2 NPs into the cells compared to Co-1 NPs. In another study, according to MTT results, polycaprolactone nanoparticles loaded with PTX and coated with P188 showed more cytotoxic effects compared to uncoated nanoparticles [29]. The results of the present study demonstrate apoptosis hallmarks including fragmented DNA through DAPI staining, decreased expression of the anti-apoptotic protein Bcl-2 and disruption of the cell membranes through Annexin-V [47]. In addition, necrosis was observed for both Co-2 NPs and Co-1 NPs using PI⁺. Furthermore, the released LDH in U87 cells showed that the cell membrane integrity was disrupted during the necrosis process [48].

It is believed that most of the nanoparticles trapped by the liver and spleen via blood circulation results in an outbreak of side effects. Targeted drug delivery systems reduce toxicity and increase the accumulation of nanoparticles in the accurate site or organ of the body. There are lots of reasons which impact this phenomenon including nanoparticle size, surface modification, morphology, chemical components, etc. It seems that particles with mean diameters below 10 nm are eliminated easily by renal excretion and particles larger than 200 nm are a proper choice for the mononuclear phagocyte system.

5. Conclusion

In this study, various PLGA NPs with PVA-P188 surface modifiers, containing MTX and PTX, either alone or combined, were prepared with proper physicochemical characteristics for parenteral administration. The most desirable carrier, Co-2 NPs, entered a model glioblastoma cell, U87 MG cells, more efficiently. Besides, the apoptotic, necrotic and cytotoxic activity of Co-2 NPs on U87 MG cells were significantly superior compared to other formulations. Therefore, Co-2 NPs prepared in this study, can be a promising candidate for the treatment of brain cancer, whilst further studies on NP stability, protein corona formation and cytotoxicity in an animal model are suggested.

Declaration of competing interest

The authors declare no conflict of interest.

Acknowledgement

This work was supported by Tehran University of Medical Sciences, Grant No. 96-01-87-34138, Iran.

Appendix A. Supplementary data

Supplementary data to this article can be found online at <https://doi.org/10.1016/j.lfs.2020.117943>.

References

- [1] H. Xin, X. Sha, X. Jiang, W. Zhang, L. Chen, X. Fang, Anti-glioblastoma efficacy and safety of paclitaxel-loading Angiopep-conjugated dual targeting PEG-PCL nanoparticles, *Biomaterials* 33 (2012) 8167–8176.
- [2] F. Madani, A. Goodarzi, M. Hashemi, B. Mujokoro, M. Khosravani, M. Adabi, Preparation of methotrexate loaded PLGA nanoparticles coated with PVA and Poloxamer188, *Nanomed. Res. J.* 3 (2018) 19–24.
- [3] J. Yue, S. Liu, R. Wang, X. Hu, Z. Xie, Y. Huang, X. Jing, Transferrin-conjugated micelles: enhanced accumulation and antitumor effect for transferrin-receptor-overexpressing cancer models, *Mol. Pharm.* 9 (2012) 1919–1931.
- [4] I. Ojima, Modern molecular approaches to drug design and discovery, ACS Publications, 2008.
- [5] V. Piazzini, E. Landucci, G. Graverini, D. Pellegrini-Giampietro, A. Bilia, M. Bergonzi, Stealth and cationic nanoliposomes as drug delivery systems to increase andrographolide BBB permeability, *Pharmaceutics* 10 (2018) 128.
- [6] J. Kreuter, Mechanism of polymeric nanoparticle-based drug transport across the blood-brain barrier (BBB), *J. Microencapsul.* 30 (2013) 49–54.
- [7] A.K. Singla, A. Garg, D. Aggarwal, Paclitaxel and its formulations, *Int. J. Pharm.* 235 (2002) 179–192.
- [8] S.B. Kaye, New antimetabolites in cancer chemotherapy and their clinical impact,

- Br. J. Cancer* 78 (1998) 1.
- [9] L. Verdusco-Rodríguez, E.H. Aguirre-González, H.C. Verdusco-Aguirre, Durable complete response induced by paclitaxel-nimotuzumab-methotrexate chemotherapy in a patient with metastatic head and neck squamous cell carcinoma, *Hematol./Oncol. Stem Cell Ther.* 4 (2011) 182–184.
- [10] Y. Mi, J. Zhao, S.-S. Feng, Targeted co-delivery of docetaxel, cisplatin and herceptin by vitamin E TPGS-cisplatin prodrug nanoparticles for multimodality treatment of cancer, *J. Control. Release* 169 (2013) 185–192.
- [11] B. Mujokoro, M. Adabi, E. Sadroddiny, M. Adabi, M. Khosravani, Nano-structures mediated co-delivery of therapeutic agents for glioblastoma treatment: a review, *Mater. Sci. Eng. C* 69 (2016) 1092–1102.
- [12] X. Wan, J.J. Beaudoin, N. Vinod, Y. Min, N. Makita, H. Bludau, R. Jordan, A. Wang, M. Sokolsky, A.V. Kabanov, Co-delivery of paclitaxel and cisplatin in poly (2-oxazoline) polymeric micelles: implications for drug loading, release, pharmacokinetics and outcome of ovarian and breast cancer treatments, *Biomaterials* 192 (2019) 1–14.
- [13] B. Mujokoro, F. Madani, S.S. Esnaashari, M. Khosravani, M. Adabi, Combination and co-delivery of methotrexate and curcumin: preparation and in vitro cytotoxic investigation on glioma cells, *J. Pharm. Innov.* (2019) 1–10.
- [14] M.R. Malekpour, M. Naghibzadeh, M.R.H. Najafabadi, S.S. Esnaashari, M. Adabi, B. Mujokoro, M. Khosravani, M. Adabi, Effect of various parameters on encapsulation efficiency of mPEG-PLGA nanoparticles: artificial neural network, *Biointerface Res. Appl. Chem.* 8 (2018) 3267–3272.
- [15] M.T. Anganeh, F.S.T. Mirakabad, M. Izadi, V. Zeighamian, F. Badrzadeh, R. Salehi, N. Zarghami, M. Darabi, A. Akbarzadeh, M. Rahmati-Yamchi, The comparison between effects of free curcumin and curcumin loaded PLGA-PEG on telomerase and TRF1 expressions in calu-6 lung cancer cell line, *Int. J. Biosci.* 4 (2014) 134–145.
- [16] M. Afshari, K. Derakhshandeh, L. Hosseinzadeh, Characterisation, cytotoxicity and apoptosis studies of methotrexate-loaded PLGA and PLGA-PEG nanoparticles, *J. Microencapsul.* 31 (2014) 239–245.
- [17] C. Fonseca, S. Simoes, R. Gaspar, Paclitaxel-loaded PLGA nanoparticles: preparation, physicochemical characterization and in vitro anti-tumoral activity, *J. Control. Release* 83 (2002) 273–286.
- [18] J.T. Opferman, A. Kothari, Anti-apoptotic BCL-2 family members in development, *Cell Death Differ.* 25 (2018) 37–45.
- [19] R.M. Mainardes, M.P.D. Gremião, R.C. Evangelista, Thermoanalytical study of praziquantel-loaded PLGA nanoparticles, *Rev. Bras. Ciên. Farmacêuticas* 42 (2006) 523–530.
- [20] A.R. de Oliveira, E.F. Molina, P. de Castro Mesquita, J.L.C. Fonseca, G. Rossanezi, M. de Freitas Fernandes-Pedrosa, A.G. de Oliveira, A.A. da Silva-Júnior, Structural and thermal properties of spray-dried methotrexate-loaded biodegradable micro-particles, *J. Therm. Anal. Calorim.* 112 (2013) 555–565.
- [21] M.F. Silva, A.A.W. Hechenleitner, J.M. Irache, A.J.A.d. Oliveira, E.A.G. Pineda, Study of thermal degradation of PLGA, PLGA nanospheres and PLGA/maghemite superparamagnetic nanospheres, *Mater. Res.* 18 (2015) 1400–1406.
- [22] M. Fernandes-Silva, A.A. Winkler-Hechenleitner, J.M. Irache, A.J. Aparicio-de-Oliveira, E.A. Gomez-Pineda, Study of Thermal Degradation of PLGA, PLGA Nanospheres and PLGA/Maghemite Superparamagnetic Nanospheres, (2015).
- [23] J.G. Hiremath, N.S. Khamar, S.G. Palavalli, C.G. Rudani, R. Aitha, P. Mura, Paclitaxel loaded carrier based biodegradable polymeric implants: preparation and in vitro characterization, *Saudi Pharm. J.* 21 (2013) 85–91.
- [24] D.J. Begley, ABC transporters and the blood-brain barrier, *Curr. Pharm. Des.* 10 (2004) 1295–1312.
- [25] J.-Y. Kim, W.I. Choi, Y.H. Kim, G. Tae, Brain-targeted delivery of protein using chitosan-and RVG peptide-conjugated, pluronic-based nano-carrier, *Biomaterials* 34 (2013) 1170–1178.
- [26] M.J. Santander-Ortega, N. Csaba, L. González, D. Bastos-González, J.L. Ortega-Vinuesa, M.J. Alonso, Protein-loaded PLGA-PEO blend nanoparticles: encapsulation, release and degradation characteristics, *Colloid Polym. Sci.* 288 (2010) 141–150.
- [27] S. Gelperina, O. Maksimenko, A. Khalansky, L. Vanchugova, E. Shipulo, K. Abbasova, R. Berdiev, N. Wohlfart, N. Chepurnova, J. Kreuter, Drug delivery to the brain using surfactant-coated poly (lactide-co-glycolide) nanoparticles: influence of the formulation parameters, *Eur. J. Pharm. Biopharm.* 74 (2010) 157–163.
- [28] C.-G. Keum, Y.-W. Noh, J.-S. Baek, J.-H. Lim, C.-J. Hwang, Y.-G. Na, S.-C. Shin, C.-W. Cho, Practical preparation procedures for docetaxel-loaded nanoparticles using polylactic acid-co-glycolic acid, *Int. J. Nanomedicine* 6 (2011) 2225.
- [29] Y. Zhang, L. Tang, L. Sun, J. Bao, C. Song, L. Huang, K. Liu, Y. Tian, G. Tian, Z. Li, A novel paclitaxel-loaded poly (ϵ -caprolactone)/poloxamer 188 blend nanoparticle overcoming multidrug resistance for cancer treatment, *Acta Biomater.* 6 (2010) 2045–2052.
- [30] H. Fessi, F. Puisieux, J.P. Devissaguet, N. Ammouy, S. Benita, Nanocapsule formation by interfacial polymer deposition following solvent displacement, *Int. J. Pharm.* 55 (1989) R1–R4.
- [31] F. Danhier, N. Lecourtier, B. Vroman, C. Jérôme, J. Marchand-Brynaert, O. Feron, V. Pr at, Paclitaxel-loaded PEGylated PLGA-based nanoparticles: in vitro and in vivo evaluation, *J. Control. Release* 133 (2009) 11–17.
- [32] S.K. Sahoo, J. Panyam, S. Prabha, V. Labhasetwar, Residual polyvinyl alcohol associated with poly (D, L-lactide-co-glycolide) nanoparticles affects their physical properties and cellular uptake, *J. Control. Release* 82 (2002) 105–114.
- [33] R.S. Kalhapure, D.R. Sikwal, S. Rambharose, C. Mocktar, S. Singh, L. Bester, J.K. Oh, J. Renukuntla, T. Govender, Enhancing targeted antibiotic therapy via pH responsive solid lipid nanoparticles from an acid cleavable lipid, *Nanomedicine* 13 (2017) 2067–2077.
- [34] W. Zhu, J. Lu, L. Dai, Multifunctional pH-responsive sprayable hydrogel based on chitosan and lignin-based nanoparticles, *Part. Part. Syst. Charact.* 35 (2018)

- 1800145.
- [35] B.S. Zolnik, D.J. Burgess, Effect of acidic pH on PLGA microsphere degradation and release, *J. Control. Release* 122 (2007) 338–344.
- [36] A. Kumari, S.K. Yadav, S.C. Yadav, Biodegradable polymeric nanoparticles based drug delivery systems, *Colloids Surf. B: Biointerfaces* 75 (2010) 1–18.
- [37] Y. Cui, Q. Xu, P.K.-H. Chow, D. Wang, C.-H. Wang, Transferrin-conjugated magnetic silica PLGA nanoparticles loaded with doxorubicin and paclitaxel for brain glioma treatment, *Biomaterials* 34 (2013) 8511–8520.
- [38] J. Guo, X. Gao, L. Su, H. Xia, G. Gu, Z. Pang, X. Jiang, L. Yao, J. Chen, H. Chen, Aptamer-functionalized PEG–PLGA nanoparticles for enhanced anti-glioma drug delivery, *Biomaterials* 32 (2011) 8010–8020.
- [39] J. Lehar, A.S. Krueger, W. Avery, A.M. Heilbut, L.M. Johansen, E.R. Price, R.J. Rickles, G.F. Short III, J.E. Staunton, X. Jin, Synergistic drug combinations tend to improve therapeutically relevant selectivity, *Nat. Biotechnol.* 27 (2009) 659.
- [40] H. Wang, Y. Zhao, Y. Wu, Y.-I. Hu, K. Nan, G. Nie, H. Chen, Enhanced anti-tumor efficacy by co-delivery of doxorubicin and paclitaxel with amphiphilic methoxy PEG-PLGA copolymer nanoparticles, *Biomaterials* 32 (2011) 8281–8290.
- [41] K.P. Musmade, P.B. Deshpande, P.B. Musmade, M.N. Maliyakkal, A.R. Kumar, M.S. Reddy, N. Udupa, Methotrexate-loaded biodegradable nanoparticles: preparation, characterization and evaluation of its cytotoxic potential against U-343 MG human neuronal glioblastoma cells, *Bull. Mater. Sci.* 37 (2014) 945–951.
- [42] A. des Rieux, V. Fievez, M. Garinot, Y.-J. Schneider, V. Préat, Nanoparticles as potential oral delivery systems of proteins and vaccines: a mechanistic approach, *J. Control. Release* 116 (2006) 1–27.
- [43] M. Saad, O.B. Garbuzenko, T. Minko, Co-delivery of siRNA and an Anticancer Drug for Treatment of Multidrug-resistant Cancer, (2008).
- [44] S.-M. Tu, E. Hossan, R. Amato, R. Kilbourn, C.J. Logothetis, Paclitaxel, cisplatin and methotrexate combination chemotherapy is active in the treatment of refractory urothelial malignancies, *J. Urol.* 154 (1995) 1719–1722.
- [45] Y.A. Yeh, E. Olah, J.J. Wendel, G.W. Sledge Jr., Synergistic action of taxol with tiazofurin and methotrexate in human breast cancer cells: schedule-dependence, *Life Sci.* 54 (1994) PL431–PL435.
- [46] L. Gianni, J. Baselga, W. Eiermann, V.G. Porta, V. Semiglazov, A. Lluch, M. Zambetti, D. Sabadell, G. Raab, A.L. Cussac, Phase III trial evaluating the addition of paclitaxel to doxorubicin followed by cyclophosphamide, methotrexate, and fluorouracil, as adjuvant or primary systemic therapy: European Cooperative Trial in Operable Breast Cancer, *J. Clin. Oncol.* 27 (2009) 2474–2481.
- [47] Z. Bacsó, R.B. Everson, J.F. Eliason, The DNA of annexin V-binding apoptotic cells is highly fragmented, *Cancer Res.* 60 (2000) 4623–4628.
- [48] V. Bhardwaj, D. Ankola, S. Gupta, M. Schneider, C.-M. Lehr, M.R. Kumar, PLGA nanoparticles stabilized with cationic surfactant: safety studies and application in oral delivery of paclitaxel to treat chemical-induced breast cancer in rat, *Pharm. Res.* 26 (2009) 2495–2503.